



1 **Time series of Inland Surface Water Dataset in China (ISWDC) for 2000-2016**

2 **derived from MODIS archives**

3 Shanlong Lu¹, Jin Ma^{1,2}, Xiaoqi Ma^{1,3}, Hailong Tang^{1,4}, Hongli Zhao⁵, Muhammad Hasan Ali Baig⁶

4 ¹Key Laboratory of Digital Earth Science, State Key Laboratory of Remote Sensing Science, Institute of Remote Sensing and Digital Earth,
5 Chinese Academy of Sciences, Beijing 100094, China;

6 ²College of Information Science and Engineering, Shandong Agricultural University, Tai'an 271018, China;

7 ³School of Earth Sciences and Resources, China University of Geosciences, Beijing 100083, China;

8 ⁴College of Earth Science, Chengdu University of Technology, Chengdu 610059, China;

9 ⁵State key Laboratory of Simulation and Regulation of Water Cycle in River Basin, China Institute of Water Resources and Hydropower
10 Research, Beijing 100038, China;

11 ⁶Institute of Geo-Information & Earth-Observation (IGEO), PMAS Arid Agriculture University Rawalpindi, Rawalpindi 46300, Pakistan.

12 Correspondence to: Shanlong Lu (lusl@radi.ac.cn)

13

14 **Abstract.** The moderate spatial resolution and high temporal resolution of the MODIS imagery make it an ideal
15 resource for the time series surface water monitoring and mapping. We used MODIS MOD09Q1 surface reflectance
16 archive images to create Inland Surface Water Dataset in China (ISWDC), which maps the water body larger than
17 0.0625 km² in the terrestrial land of China for the period 2000–2016, in 8-day temporal and 250 m spatial resolution.
18 We assessed the accuracy of the ISWDC by comparing with the national land cover derived surface water data and the
19 Global Surface Water (GSW) data. The results show that the ISWDC is closely correlated with the national reference
20 data with the determinant coefficients (R^2) greater than 0.99 in 2000, 2005, and 2010, while the ISWDC has similar
21 spatial patterns in different regions with the GSW data set in 2015 too. The ISWDC data set can be used for studies on
22 the inter-annual and seasonal variation of the surface water systems. It can also be used as reference data for other
23 surface water data set verification and as input parameter for regional and global hydro-climatic models. The ISWDC
24 data are available at <http://doi.org/10.5281/zenodo.1463694>.



1 Introduction

2 Surface water is the most important source of water from planetary water resources available for the
3 survival of both human and ecological systems in sustainable environment. It is a key component of the
4 hydrological cycle and the key factor affecting sustainable development of human society and
5 ecosystem. Both climate change and human activities has a role in affecting and modifying the location
6 and persistence of the surface water. In order to locate the position and examine the change in dynamics
7 of the inland surface water, regional and global data sets have already been produced through remote
8 sensing data by various researchers (Carroll et al., 2009; Verpoorter et al., 2014; Feng et al., 2015; Klein
9 et al., 2014; Tulbure et al., 2016). But these contemporary researches did limited exploration for
10 measuring long-term changes at high spatial and temporal resolution. Pekel et al. (2016) quantified the
11 changes in global surface water (GSW) over the past 32 years (1984-2015) at 30-metre resolution by
12 using the Landsat satellite images. Klein et al. (2017) generated a 250 m daily global dataset of inland
13 water bodies based on a combination of MODIS Terra and Aqua daily classifications. However, the
14 temporal resolution of the former research is near monthly, and the latter research only produced data
15 sets of 2013-2015.

16 In China numerous regional case studies have been done and produced some surface water data sets
17 but in bits and pieces (Du et al., 2012; Lai et al., 2013; Luo et al., 2017). Their research hotspot was
18 Qinghai-Tibetan Plateau due to the existence of the largest number of inland lakes there with the highest
19 elevation on the planet (Lu et al., 2017). Several research groups are focusing on the lake water changes
20 of this region. Almost every 10-year of lake water surface area datasets from 1960s to present has been
21 produced (Song et al., 2014; Zhang et al., 2014, 2017; Wan et al., 2014, 2016). At the national scale, the
22 national wetland remote sensing datasets in 1978, 1990, 2000 and 2008 (Niu et al., 2012), the national
23 land cover datasets in 1990, 2000, 2010, and 2015 (Wu et al., 2017), and the national land use datasets
24 in 1990, 1995, 2000, 2005, 2010, 2015 (Liu et al., 2018) contain the inter-decadal or 5-year time scale



1 water surface dataset. However, these datasets have limited temporal resolution and not freely and fully
2 shared.

3 The most commonly used method of water extraction is water index method, such as Normalized
4 Difference Water Index (NDWI) (Rogers and Kearney, 2004), Modified Normalized Difference Water
5 Index (MNDWI) (Xu, 2006), and Automated Water Extraction Index (AWEI) (Feyisa, et al., 2018).
6 Furthermore, the single band threshold segmentation method (Li et al., 2012, Lu et al., 2017) and the
7 multiband threshold segmentation method (Pekel et al. 2014) are also in practice. The key step for using
8 these methods to extract water boundary is to determine the threshold value for segmentation. The
9 existing threshold determination methods include human visual judgment (Huang et al., 2008; Li et al.,
10 2012) and sample statistical analysis (Feyisa et al, 2014; Pekel etc., 2014; Pekel et al., 2016). The
11 former relies on subjective experience, causes the extraction results to be unstable, and it is difficult to
12 apply to large scale and large amount of data research. Although the latter can get more accurate results
13 through extensive sampling statistics, the use of a unified threshold for whole image or whole region
14 may produce large errors in the local area. In order to overcome these problems, various comprehensive
15 classification methods are widely used. Verpoorter et al. (2014) combined the Principal Component
16 Analysis (PCA) and the Modified Brightness Index (MBI) to generate supervised classes, and divided it
17 into water and non-water regions by using the decision tree method. Pekel et al. (2016) proposed an
18 expert system by synthetic use of visual analytical spectral library, NDVI index, HSV transformation
19 results, and decision tree method. Khandelwal et al. (2017) introduced a global supervised classification
20 based approach by defining initial spatial extents of each water body, using the global sample datasets,
21 and incorporating all the spectral reflectance bands of the MODIS images. Use of supervised
22 classification and decision tree method may improve the accuracy of water surface boundary extraction,
23 however it increases the difficulty and efficiency of the method at the same time. Zhang et al. (2017)
24 proposed an automatic threshold determination method based on the LBV transformation of Landsat 8
25 OLI surface reflectance images. It was verified as an accurate, simple, and robust method for surface



1 water extraction. However, the cloud pixels and atmospheric correction influences are not considered.

2 China is one of the most rivers and lakes in the world. There are more than 1500 rivers with an area
3 exceeding 1000 km², and 2928 lakes with an area larger than 1 km² and a total area of 91,020 km² (Ma
4 et al. 2011). However, due to the influence of geography and monsoon climate, these surface water
5 resources are very uneven in distribution. They are found more in the South than in the North, and more
6 in the East than in the West. With the development of the economy, the increase in the demand for
7 industrial, agricultural and domestic water has brought great pressure to these surface water systems,
8 especially during the irrigation and drought season (Gong et al., 2011; Barnett et al., 2015). However,
9 until now, there exists no single data set that can fully reflect both the spatial distribution characteristics
10 and time variations of surface water in China. So the research to investigate the relationship between the
11 national surface water and the global climate and human activities is limited.

12 Therefore, in order to address these limitations and to fulfill the research need to develop
13 comprehensive dataset both spatially and temporally, this paper presents the Inland Surface Water
14 Dataset in China (ISWDC) during the period of 2000-2016, which is derived from the 8-day and 250 m
15 spatial resolution MODIS MOD09Q1 product. After recalling the methodology used in surface water
16 mapping from the MODIS MOD09Q1 as described by Lu et al. (2017), the precision and accuracy of
17 the data set are reported, including the cross comparison with other national and global data sets.

18

19 **2 Study area and data**

20 The inland water of this data set refers to the water body larger than 0.0625 km² of the terrestrial land of
21 China. The MODIS MOD09Q1 imagery has been used to extract surface water
22 (<https://ladsweb.modaps.eosdis.nasa.gov/search/>). MOD09Q1 is a MODIS level 3 land surface
23 reflectance product. It is an 8 day synthetic imagery of Band 1 (red band) and Band 2 (near-infrared
24 band) with the spatial resolution of 250 m. In this study the near-infrared band is directly used to extract



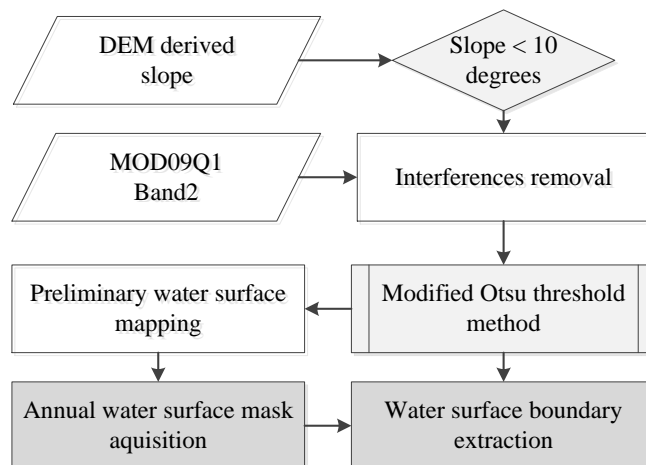
1 the surface water. There are 22 scenes covering the whole territory of China for single date in a form of
2 mosaic. For the complete temporal coverage from February 24, 2000 to December 26, 2016, total 16698
3 images were used. The SRTM (Shuttle Radar Topography Mission) DEM data with 90 m spatial
4 resolution is used as an ancillary data for surface water extraction, which is jointly measured by
5 NASA-JPL (NASA Jet Propulsion Laboratory) and NIMA (National Imagery and Mapping Agency
6 (Slater et al., 2006).

7 Two types of reference data set are used for cross comparison. The first one is a derived sub-dataset
8 of surface water from China national 30 m land cover data set of 2000, 2005 and 2010 (Liu et al., 2014;
9 Wu et al. 2017). The second one is the global surface water (GSW) at 30 meter resolution for
10 2000-2015 produced by Pekel et al. (2016).

11

12 3 Methods

13 The single band one by one water body threshold segmentation method proposed by Lu et al. (2017) is
14 used to extract the surface water boundary, which includes four steps: interferences removal,
15 preliminary water surface mapping, annual water surface mask acquisition, and water surface boundary
16 extraction (Figure 1). In this study the last two steps are updated and improved as follows.



17



Figure 1 Flowchart of the water surface extraction method reference to Lu et al. (2017)

3.1 Annual water surface mask acquisition

The water surface mask is a key input data for excluding land disturbance factors that affect the extraction of water surface boundary. It is generated from the preliminary water surface mapping results based on the selected images having lesser cloud and better quality in each year, by applying modified Otsu threshold method (Lu et al., 2017). In order to eliminate error in water area information caused by the cloud and cloud shadows in this process, the determination probability (p) parameter is used based on the fact that the cloud and its shadow will not appear in the same position over longer time periods. The equation is as follows,

$$\text{if } \sum_{i=1}^n d_i \geq n \times p, D=1$$

where n is the number of the preliminary water surface mapping images, d_i is the pixel value of image i , D is the pixel value of the annual water surface mask, p is the determination probability for identifying water pixel. Table 1 shows the images used for annual water surface mask generation and the determination probability for each year, which were visually selected and determined based on the size of the water bodies and the ratio of the cloud cover in the whole image. The images with relatively larger water body areas and little cloud cover were finally chosen. The determination probability (p) was determined based on the cloud and its shadow elimination effect (Lu et al., 2017).

Table 1 the images used for annual water surface mask generation and the determination probability each year

Year	Selected 8-day image dates (DOY)	Determination probability (p)
2000	185, 201, 209, 233, 241, 249, 257, 265, 281, 305	0.2
2001	185, 193, 201, 233, 241, 249, 257, 265, 273, 281	0.2
2002	185, 193, 209, 217, 225, 233, 241, 249, 257, 265	0.2
2003	177, 193, 201, 209, 217, 233, 249, 257, 265, 289	0.3
2004	185, 201, 217, 225, 233, 249, 257, 265, 273, 281	0.2

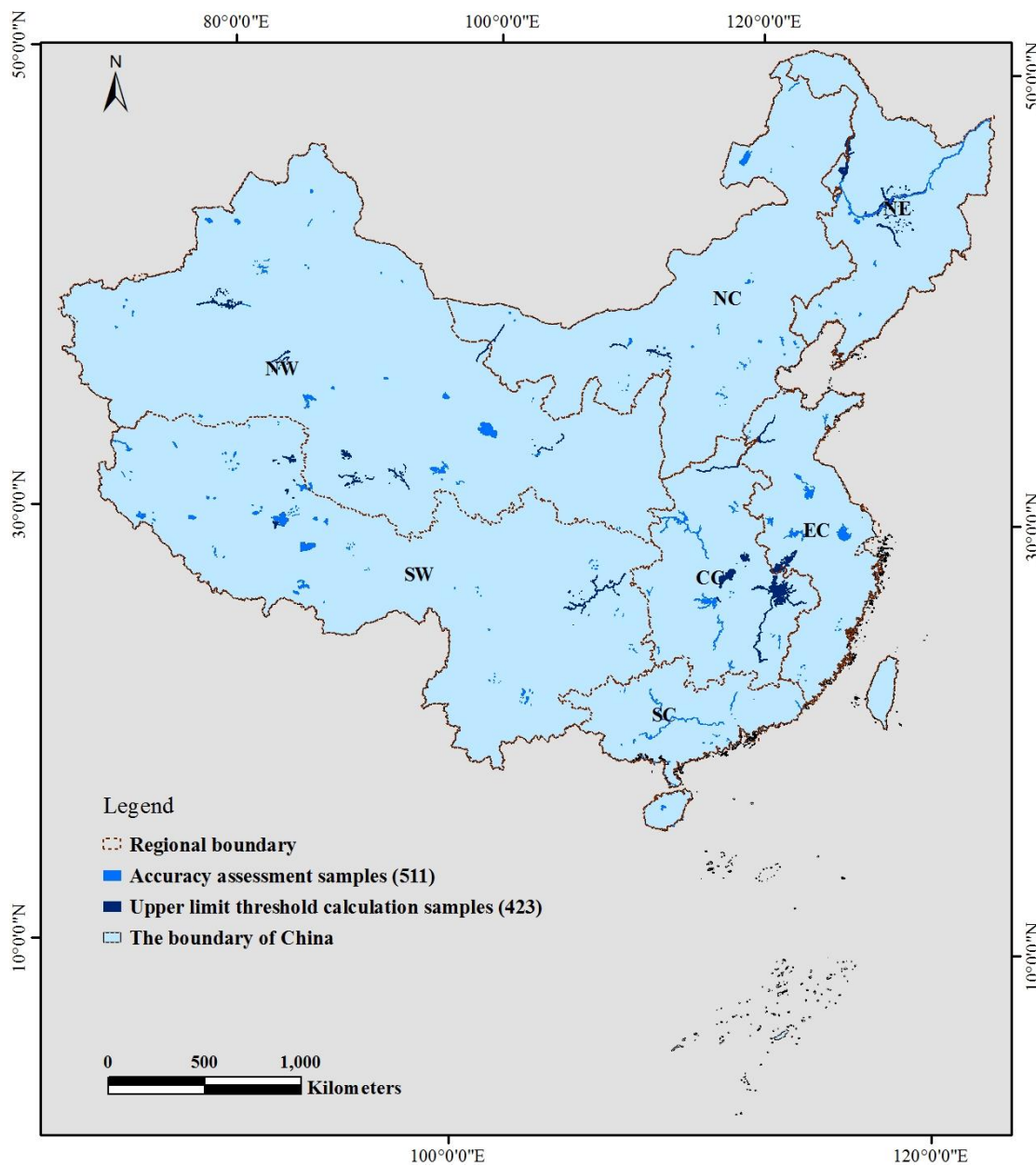


2005	209、217、225、233、241、249、257、265、273、281	0.2
2006	137、145、169、177、185、193、201、209	0.2
2007	185、193、201、209、217、225、233、241、257、265	0.3
2008	193、201、209、225、233、241、249、257、265、273	0.3
2009	129、137、153、169、185、193、201、233、241、249	0.3
2010	185、209、217、225、233、241、249、257、273、281	0.2
2011	161、169、177、185、201、209、217、225、233、265	0.2
2012	185、201、209、217、225、233、241、257、265、273	0.2
2013	185、193、201、209、217、225、233、249、257、281	0.2
2014	193、201、209、225、233、241、249、265、257、273	0.3
2015	201、209、217、241、249、257、265、273、281、28	0.2
2016	193、209、225、241、257、265、273、289、305	0.2

1

2 **3.2 Water surface boundary extraction**

3 Before determining the threshold value for each water body, the average pixel value in the mask area is
 4 used to eliminate the influence of the land pixels (Lu et al., 2017). Although this method can improve
 5 the accuracy of water surface extraction, the average pixel value in different season will be different. In
 6 order to solve this problem, 423 sample lakes and rivers in different regions of the country are selected
 7 (Figure 2) to obtain the reference average pixel value in different season. Two images with lesser clouds
 8 are selected for each season in each year, and the average pixel values of spring, summer, and autumn
 9 are calculated based on the water body samples. They were used as the upper limit threshold for
 10 extracting the water surface boundaries. Due to the smaller difference between the pixel values of ice
 11 layer and the water surface in winter, the average pixel value will cause the ice layer to be extracted as
 12 water surface, the minimum pixel value of the samples are used as the upper limit threshold for water
 13 surface boundary extraction in winter.



1

2 **Figure 2** The boundary of China, the accuracy assessment and the upper limit threshold calculation samples for
3 surface water extraction. NW: Northwest China, SW: Southwest China, SC: South China, CC: Central China; NC:
4 North China, NE: Northeast China, EC: East China.

5

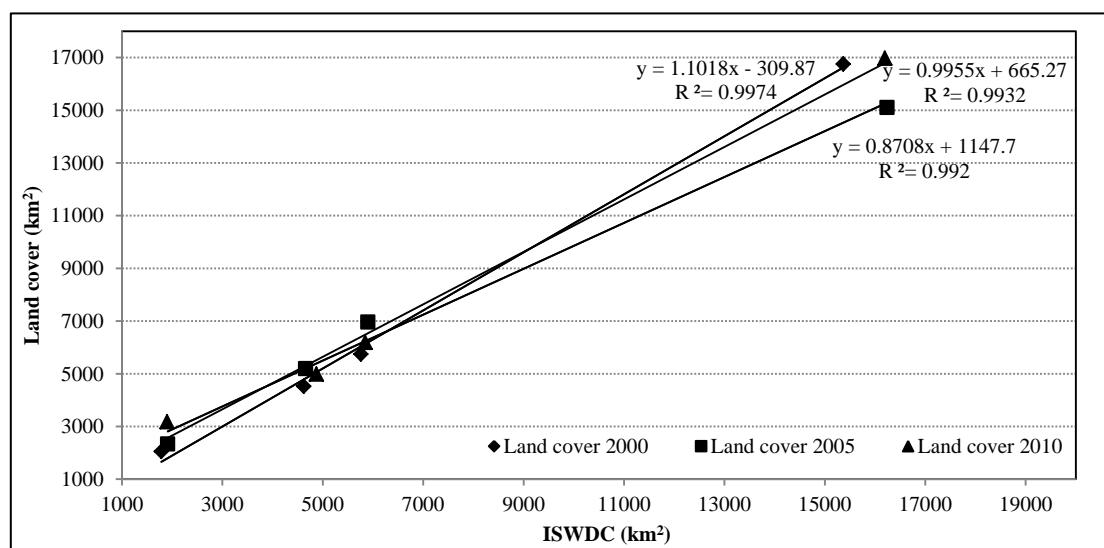


1 4 Accuracy assessment

2 4.1 Comparison with the national land cover data set

3 Based on the 30 m resolution national land cover data set of 2000, 2005, and 2010, 511 lake and river
4 samples from different regions are selected as ground truth data (Figure 2), including 11 very large
5 water bodies with areas larger than 1000 km², 12 large water bodies with areas larger than 500 km² and
6 less than 1000 km², 29 medium size water bodies with area larger than 100 km² and less than 500 km²,
7 and 459 small water bodies with area less than 100 km². They were compared with the maximum
8 ISWDC in the corresponding years.

9 The results shows that the ISWDC are in high consistency with the reference land cover derived
10 surface water data. The determinant coefficients (R^2) in 2000, 2005 and 2010 are 0.9974, 0.992, and
11 0.9932 respectively (Figure 3). The confusion matrix analysis results show that the average user
12 accuracy is 91.13%, the average producer accuracy is 88.95%, and the average Kappa coefficient is 0.88
13 in three years (Table 2).



14
15 **Figure 3 Comparison of the total area of surface water body samples with different size (< 100 km², 100-500 km², 500-1000**
16 **km², >1000 km²) between ISWDC and the National land cover derived surface water data.**



1

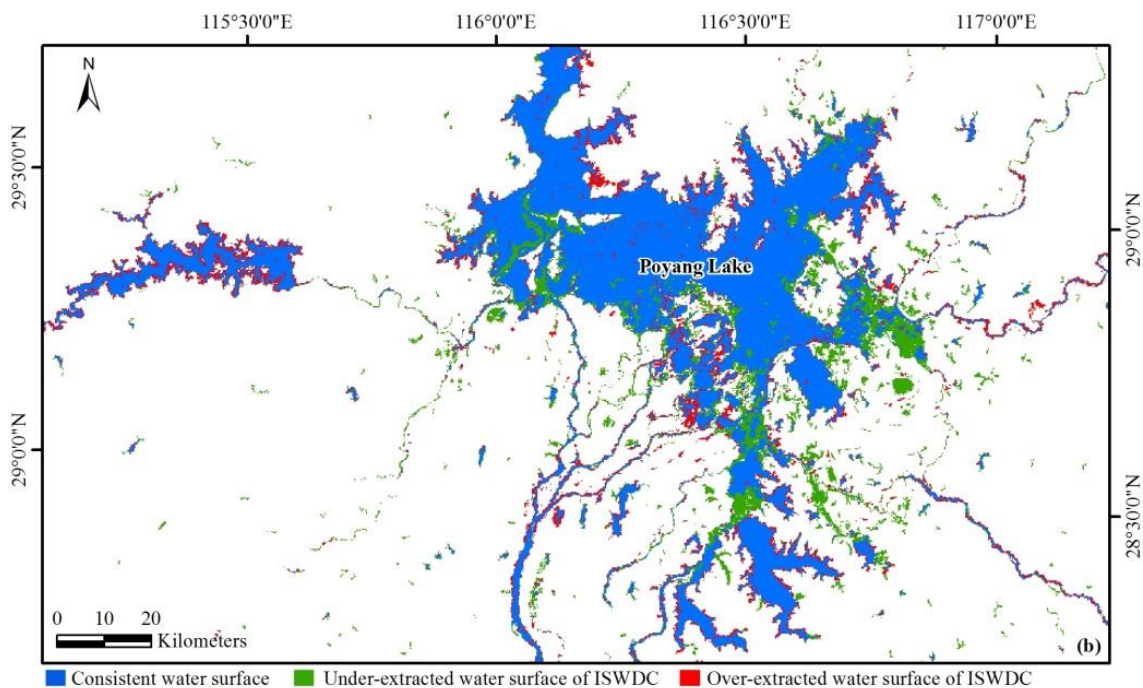
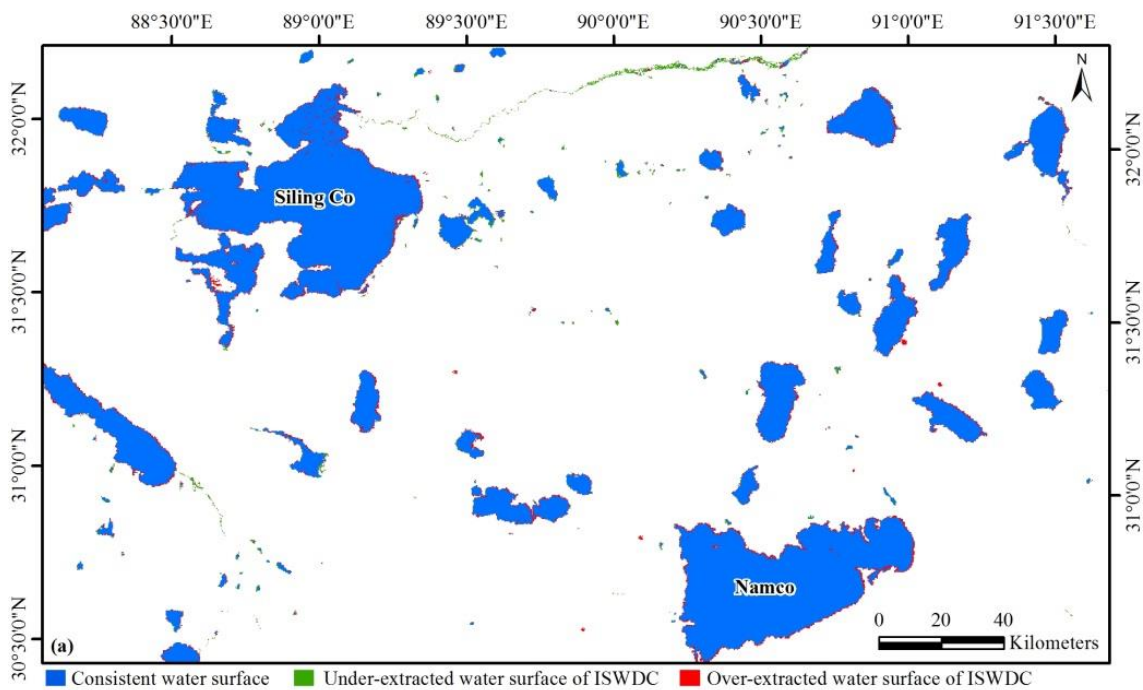
Table 2 Accuracy analysis samples in different region and the assess results

Sample regions	Sample water bodies				
	Very large	Large	Medium	Small	Total
North China (NC)	1	1	1	73	76
Northeast China (NE)	1	2	2	21	26
East China (EC)	2	1	3	34	40
Southwest China (SW)	2	3	5	75	85
Northwest China (NW)	2	2	13	166	183
Central China (CC)	2	1	2	46	51
South China (SC)	1	2	3	44	50
Average user accuracy	96.14	94.75	93.69	79.96	91.13
Average producer accuracy	92.64	88.87	92.69	81.60	88.95
Average Kappa coefficient	0.94	0.93	0.93	0.72	0.88

2

3 **4.2 Assessment against the global surface water data set**

4 The annual ISWDC and GSW permanent water bodies with area larger than 0.0625 km² in 2015 are
 5 presented in Figure 4. Our results also indicate similar spatial patterns in different regions. For the lake
 6 groups in central Qinghai-Tibetan Plateau, the comparison between ISWDC obtained from MODIS and
 7 Landsat derived GSW indicated a closer pattern between the two results (Figure 4a). For the rivers and
 8 lakes interlaced Poyang Lake region, in addition to the narrow width of the river and some small water
 9 bodies, the coincidence between the two data sets is also very high (Figure 4b). The over-extracted
 10 water (red regions in Figure 4) on the margins for large water bodies like Siling Co, Namco, Poyang
 11 Lake, and some of the wide rivers, and the under-extracted slender rivers and small water bodies (green
 12 regions in Figure 4), for the ISWDC data set, are mainly caused by the mixed pixel effects due to
 13 relatively coarse spatial resolution of the MODIS images.



3 **Figure 4 Comparison of permanent water derived from ISDWC and GSW over the sites of the central Qinghai-Tibetan Plateau (a)**
4 **and Poyang Lake region (b).**



1 **5 Applications and data availability**

2 **5.1 Time series surface water data set applications**

3 The time series surface water data set can be used to analyze the inter-annual and seasonal variation
4 characteristics of surface water area, such as inter-annual variation trend, abrupt change time,
5 intra-annual hydrological process monitoring and so on (Huang et al., 2018; Xing et al., 2018).
6 Similarly, it can be used as a cross-validation reference data for global surface water data sets with
7 similar spatial resolution (Klein et al., 2017), and as a key input parameter for regional and global
8 hydro-climatic models' calibration and evaluation (Khan et al., 2011; Stacke and Hagemann, 2012).

9 Based on the ISDWC from 2000-2016, the spatial distributions of surface water can be clearly
10 depicted by means of multi-year average analysis. The results in Table 3 show that surface water of
11 inland China is mainly distributed in the western China, accounting for 49.13% of the total surface
12 water area, with 29.88% in the Southwest China (SW) and 19.25% in the Northwest China (NW),
13 followed by the Central China (CC) and East China (EC), which accounted for 8.13% and 24.78% of
14 the total surface water area respectively. The North China (NC), Northeast China (NE) and South China
15 (SC) account for the other 17.96% of the national surface water area. In addition, the time series of
16 water surface data can also be used to delineate the annual variation of surface water, such as the annual
17 maximum and minimum water surface occurrence time (Figure 5) and lake freezing and thawing
18 process (Figure 6).

19 **Table 3 The average distribution of surface water area in inland China in 2000-2016**

Regions	Area(km ²)	Area percentage (%)
North China (NC)	6250.6	6.11
Northeast China (NE)	8991.3	8.79
East China (EC)	25342.3	24.78
Central China (CC)	9313.4	8.13



South China (SC)	3126.0	3.06
Southwest China (SW)	30548.6	29.88
Northwest China (NW)	19680.2	19.25
Total	103252.3	100.00

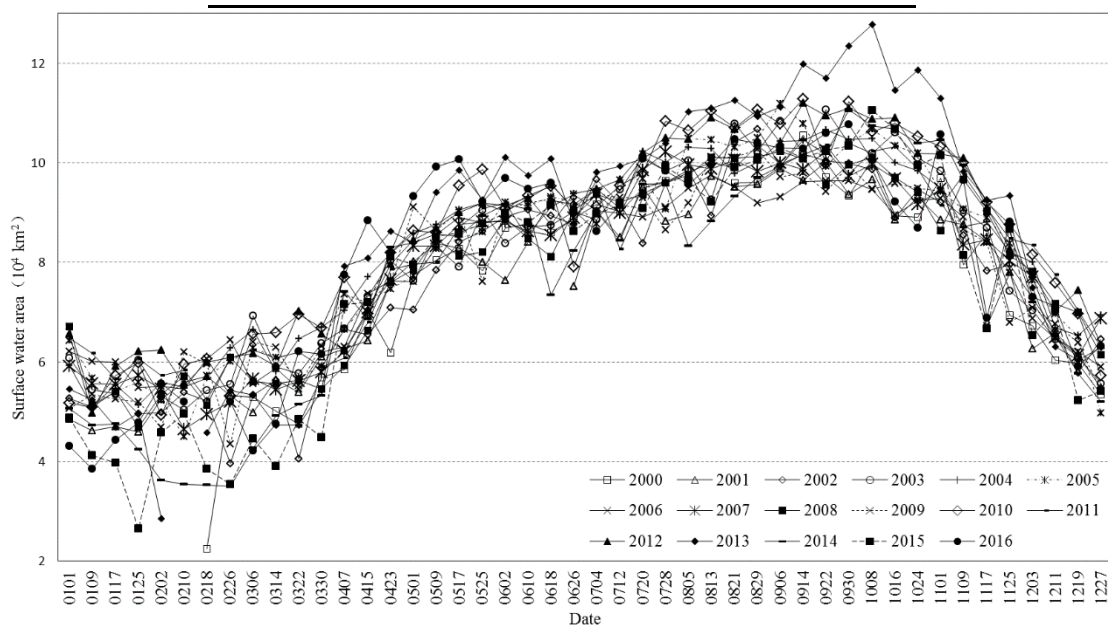


Figure 5 Annual change of total water area during the period of 2000-2016.

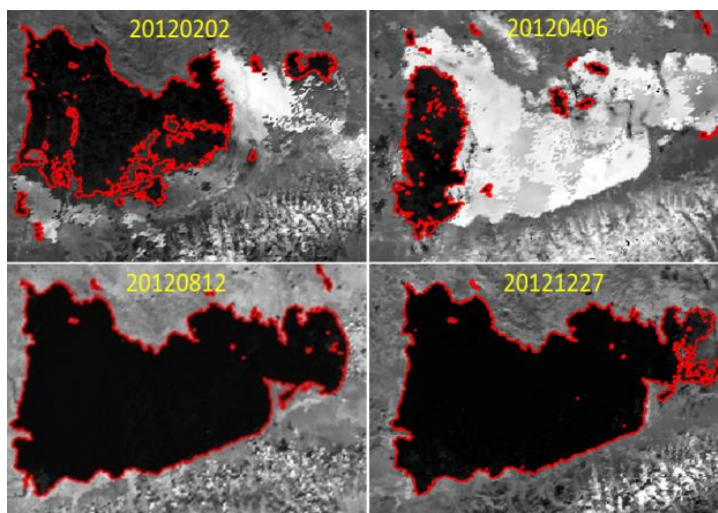


Figure 6 Freezing and thawing condition in different dates of Namco Lake in 2012



1 **5.2 Data availability**

2 The ISDWC data set is distributed under a Creative Commons Attribution 4.0 License. The data may be
3 downloaded from the data repository Zenodo at <http://doi.org/10.5281/zenodo.1463694> (Lu et al., 2018).
4 In each 8-day surface water image, the pixel values of 1 and 0 represent the water and the background
5 respectively. The 8-day data in each month can be used to calculate the monthly water occurrence and
6 all the 8-day data in each year can be used to calculate the yearly water occurrence, by summing up all
7 the surface water image together in corresponding time periods.

8

9 **6. Conclusions**

10 In this study, the 8-day 250-meter resolution surface water data set of inland China (ISDWC) from 2000
11 to 2016 was introduced. It is a long time series and consistent spatial resolution, which solves the
12 problem of lack of surface water area data set with long time series in China.

13 The accuracy analysis results show that the ISWDC are in high consistency with the national land
14 cover derived surface water data in 2000, 2005 and 2010, with the determinant coefficients (R^2) of
15 0.9974, 0.992, and 0.9932 respectively. The average user accuracy is 91.13%, the average producer
16 accuracy is 88.95%, and the average Kappa coefficient is 0.88 in three years. Furthermore, the ISWDC
17 in 2015 has similar spatial patterns in different regions (including the central Qinghai-Tibetan Plateau
18 and Poyang Lake region) with the GSW data set, especially for the large water bodies (as lakes and
19 reservoirs) and the wide rivers.

20 Based on the ISDWC of 2000-2016, the spatial distribution characteristics and temporal variation
21 process of surface water can be described through the multi-year average spatial statistics and annual
22 data overlapping analysis. In addition, the data set can also be used as a cross-validation reference data
23 for other global surface water data sets, and a key input parameter for regional and global
24 hydro-climatic models.



1 **Author contributions.** SL supervised the downloading and processing of satellite images and designed the
2 methodology. JM contributed to downloading, processing satellite images, and extracting the surface water data
3 (ISDWC). XM extracted the reference surface water data from the national land cover data sets and analyzed the
4 accuracy of the ISDWC. HT extracted the Global Surface Water (GSW) from the Google Earth Engine platform. HL
5 made contribution for manuscript structure design and revision. All authors have read and approved the final paper.

6
7 **Acknowledgements.** We thank the Key Program of the National Natural Science Foundation of China (91637209),
8 the National Key Research and Development Program of China (2017YFC0405802, 2016YFC0503507-03), and the
9 Strategic Priority Research Program of the Chinese Academy of Sciences (XDA19070201) for financial support. We
10 thank NASA EOSDIS LAADS DAAC platform (<https://ladsweb.modaps.eosdis.nasa.gov/>) and NASA-JPL and NIMA
11 for providing the MODIS and SRTM data sets. We also thank JRC and Google Earth Engine
12 (<https://earthengine.google.com>) for providing the Global Surface Water (GSW) data set.

13 14 **References**

- 15 Barnett, J., Rogers, S., Webber, M., Finlayson, B., and Wang, M.: Transfer project cannot meet China's water needs,
16 *Nature*, 527, 295–297, <https://doi.org/10.1038/527295a>, 2015.
- 17 Carroll, M.L., Townshend, J.R., DiMiceli, C.M., Noojipady, P., and Sohlberg, R.A.: A new global raster water mask at
18 250 m resolution, *International Journal of Digital Earth*, 2, 291–308, <http://dx.doi.org/10.1080/17538940902951401>,
19 2009.
- 20 Du, Z., Bin, L., Ling, F., Li, W., Tian, W., Wang, H., Gui, Y., Sun, B., and Zhang, X.: Estimating surface water area
21 changes using time-series Landsat data in the Qingjiang River Basin, China, *Journal of Applied Remote Sensing*, 6,
22 3609, <https://doi.org/10.1117/1.JRS.6.063609>, 2012.
- 23 Feng, M., Sexton, J.O., Channan, S., and Townshend, J.R.: A global, high-resolution (30-m) inland water body dataset
24 for 2000: first results of a topographic–spectral classification algorithm, *International Journal of Digital Earth*, 1–21,
25 <http://dx.doi.org/10.1080/17538947.2015.1026420>, 2015.
- 26 Feyisa, G.L., Meilby, H., Fensholt, R. and Proud, S. R.: Automated Water Extraction Index: A new technique for



- 1 surface water mapping using Landsat imagery, *Remote Sensing of Environment*, 140, 23–35,
2 <http://dx.doi.org/10.1016/j.rse.2013.08.029>, 2014.
- 3 Gong, P., Yin, Y., and Yu, C.: China: Invest Wisely in Sustainable Water Use, *Science*, 331, 1264–1265,
4 <https://doi.org/10.1126/science.331.6022.1264-b>, 2011.
- 5 Huang, C., Chen, Y., Zhang, S., and Wu, J.: Detecting, extracting, and monitoring surface water from space using
6 optical sensors: A review, *Reviews of Geophysics*, 56, <https://doi.org/10.1029/2018RG000598>, 2018.
- 7 Huang, H., Zhao, P., Chen, Z., and Guo, W.: Research on the method of extracting water body information from
8 ASTER remote sensing image, *Remote Sensing Technology and Application*, 23, 525–528,
9 <https://doi.org/10.11873/j.issn.1004-0323.2008.5.525>, 2008.
- 10 Khan, S.I., Hong, Y., Wang, J., Yilmaz, K.K., Gourley, J.J., Adler, R.F., Brakenridge, G.R. Habib, S., and Irwin, D.:
11 Satellite Remote Sensing and Hydrologic Modeling for Flood Inundation Mapping in Lake Victoria Basin:
12 Implications for Hydrologic Prediction in Ungauged Basins, *IEEE TRANSACTIONS ON GEOSCIENCE AND*
13 *REMOTE SENSING*, 49, 85–95, <https://doi.org/10.1109/TGRS.2010.2057513>, 2011.
- 14 Khandelwal, A., Karpatne, A., Marlier, M.E., Kim, J., Lettenmaier, D.P., and Kumar, V.: An approach for global
15 monitoring of surface water extent variations in reservoirs using MODIS data, *Remote Sensing of Environment*, 202,
16 113–128, <http://dx.doi.org/10.1016/j.rse.2017.05.039>, 2017.
- 17 Klein, I., Dietz, A.J., Gessner, U., Galayeva, A., Myrzakhmetov, A., and Kuenzer, C.: Evaluation of seasonal water
18 body extents in Central Asia over the past 27 years derived from medium-resolution remote sensing data,
19 *International Journal of Applied Earth Observation and Geoinformation*, 26, 335–349,
20 <http://dx.doi.org/10.1016/j.jag.2013.08.004>, 2014.
- 21 Klein, I., Gessner, U., Dietz, A.J., and Kuenzer, C.: Global WaterPack – A 250 m resolution dataset revealing the daily
22 dynamics of global inland water bodies, *Remote Sensing of Environment*, 198, 345–362,
23 <http://dx.doi.org/10.1016/j.rse.2017.06.045>, 2017.
- 24 Lai, Y., Qiu, Y., Fu, W., and Shi, L.: Monitoring and analysis of surface water in Kashgar region based on TM imagery
25 in last 10 years, *Remote Sensing Information*, 28, 50–57, <https://doi.org/10.3969/j.issn.1000-3177.2013.03.009>,
26 2013.
- 27 Li, X., Xiao, J., Li, F., Xiao, R., Xu, W., and Wang, L.: Remote Sensing monitoring of the Qinghai Lake based on EOS



- 1 /MODIS data in recent 10 years, *Journal of Natural Resources*, 22, 1962–1970,
2 <http://www.jnr.ac.cn/CN/10.11849/zrzyxb.2012.11.015>, 2012.
- 3 Liu, J., Kuang, W., Zhang, Z., Xu, X., Qin, Y., Ning, J., Zhou, W., Zhang, S., Li, R., Yan, C., Wu, S., Shi, X., Jiang, N.,
4 Yu, D., Pan, X., and Chi, W.: Spatiotemporal characteristics, patterns and causes of land use changes in China since
5 the late 1980s, *ACTA GEOGRAPHICA SINICA*, 69, 3–14, <https://doi.org/10.1007/s11442-014-1082-6>, 2014.
- 6 Liu, J., Jia, N., Kuang, W., Xu, X., Zhang, S., Yan, C., Li, R., Wu, S., Hu, Y., Du, G., Chi, W., Pan, T., and Ning, J.:
7 Spatio-temporal patterns and characteristics of land-use change in China during 2010-2015, *ACTA*
8 *GEOGRAPHICA SINICA*, 73, 789–802, <https://doi.org/10.11821/dlxb201805001>, 2018.
- 9 Lu, S., Ma, J., Ma, X., Tang, H., Zhao, H., and Ali Bai Hasan, M.: Time series of Inland Surface Water Dataset in
10 China (ISWDC) [Data set], Zenodo, <http://doi.org/10.5281/zenodo.1463694>, 2018.
- 11 Lu, S., Jia, L., Zhang, L., Wei, Y., Baig, M., Zhai, Z., Ment, J., Li, X., and Zhang, G.: Lake water surface mapping in
12 the Tibetan Plateau using the MODIS MOD09Q1 product, *Remote Sensing Letters*, 8, 224–233,
13 <http://dx.doi.org/10.1080/2150704X.2016.1260178>, 2017.
- 14 Luo, C., Xu, C., Cao, Y., and Tong, L.: Monitoring of water surface area in Lake Qinghai from 1974 to 2016, *Journal*
15 *of Lake Sciences*, 29, 1245–1253, <https://doi.org/10.18307/2017.0523>, 2017.
- 16 Niu, Z., Zhang, H., Wang, X., Yao, W., Zhou, D., Zhao, K., Zhao, H., Li, N., Huang, H., Li, C., Yang, J., Liu, C., Liu,
17 S., Wang, L., Li, Z., Yang, Z., Qiao, F., Zheng, Y., Chen, Y., Sheng, Y., Gao, X., Zhu, W., Wang, W., Wang, H., Weng,
18 Y., Zhuang, D., Liu, J., Luo, Z., Cheng, X., Guo, Z., and Gong, P.: Mapping Wetland Changes in China between
19 1978 and 2008, *Chinese Science Bulletin*, 57, 1400–1411, <https://doi.org/10.1007/s11434-012-5093-3>, 2012.
- 20 Ma, R., Yang, G., Duan, H., Jiang, J., Wang, S., Feng, X., Li, A., Kong, F., Xue, B., Wu, J., and Li, S.: China's lakes at
21 present: Number, area and spatial distribution, *Science China Earth Sciences*, 394–401,
22 <https://doi.org/10.1007/s11430-010-4052-6>, 2011.
- 23 Pekel, J., Vancutsem, C., Bastin, L., Clerici, M., Vanbogaert, E., Bartholome, E., and Defourny, P.: A near real-time
24 water surface detection method based on HSV transformation of MODIS multi-spectral time series data, *Remote*
25 *Sensing of Environment*, 140, 704–716, <https://doi.org/10.1016/j.rse.2013.10.008>, 2014.
- 26 Pekel, J.F., Cottam, A., Gorelick, N., and Belward, A.S.: High-resolution mapping of global surface water and its
27 long-term changes, *Nature*, 540, 418–422, <https://doi.org/10.1038/nature20584>, 2016.



- 1 Rogers, A.S., and Kearney, M.S.: Reducing signature variability in unmixing coastal marsh Thematic Mapper scenes
2 using spectral indices, *International Journal of Remote Sensing*, 20, 2317–2335,
3 <https://doi.org/10.1080/01431160310001618103>, 2004.
- 4 Song, C., Huang, B., Ke, L., and Richards, K.S.: Remote sensing of alpine lake water environment changes on the
5 Tibetan Plateau and surroundings: A review, *ISPRS Journal of Photogrammetry and Remote Sensing*, 92, 26–37,
6 <http://dx.doi.org/10.1016/j.isprsjprs.2014.03.001>, 2014.
- 7 Stacke, T., and Hagemann, S.: Development and evaluation of a global dynamical wetlands extent scheme, *Hydrology
8 and Earth System Sciences*, 16, 2915–2933, <https://doi.org/10.5194/hess-16-2915-2012>, 2012.
- 9 Tulbure, M.G., Broich, M., Stehman, S.V., and Kommareddy, A.: Surface water extent dynamics from three decades of
10 seasonally continuous Landsat time series at subcontinental scale in a semi-arid region, *Remote Sensing
11 Environment*, 178, 142–157, <https://doi.org/10.1016/j.rse.2016.02.034>, 2016.
- 12 Verpoorter, C., Kutser, T., and Tranvik, L.: Automated mapping of water bodies using Landsat multispectral data,
13 *Limnology and Oceanography: Methods*, 10, 1037–1050, <https://doi.org/10.4319/lom.2012.10.1037>, 2012.
- 14 Verpoorter, C., Kutser, T., Seekell, D.A., and Tranvik, L.J.: A global inventory of lakes based on high-resolution
15 satellite imagery, *Geophysical Research Letters*, 41, 6396–6402, <https://doi.org/10.1002/2014GL060641>, 2014.
- 16 Wan, W., Xiao, P., Feng, X., Li, H., Ma, R., Duan, H., and Zhao, L.: Monitoring lake changes of Qinghai-Tibetan
17 Plateau over the past 30 years using satellite remote sensing data, *Chinese Science Bulletin*, 59, 1021–1035,
18 <https://doi.org/10.1007/s11434-014-0128-6>, 2014.
- 19 Wan, W., Long, D., Hong, Y., Ma, Y., Yuan, Y., Xiao, P., Duan, H., Han, Z., and Gu, X.: A lake data set for the Tibetan
20 Plateau from the 1960s, 2005, and 2014, *Scientific data*, 3, 160039, <https://doi.org/10.1038/sdata.2016.39>, 2016.
- 21 Wang, J., Sheng, Y. and Tong, T.S.D.: Monitoring decadal lake dynamics across the Yangtze Basin downstream of
22 Three Gorges Dam, *Remote Sensing of Environment*, 152, 251–269, <https://doi.org/10.1016/j.rse.2014.06.004>,
23 2014.
- 24 Wang, X., Xie, S., Zhang, X., Chen, C., Guo, H., Du, J., and Duan, Z.: A robust Multi-Band Water Index (MBWI) for
25 automated extraction of surface water from Landsat 8 OLI imagery, *International Journal of Applied Earth
26 Observation and Geoinformation*, 68, 73–91, <https://doi.org/10.1016/j.jag.2018.01.018>, 2018.
- 27 Wu, B., Bao, A., Chen, J., Huang, J., Li, A., Liu, C., Ma, R., Wang, Z., Yan, C., Yu, X., Zeng, Y., and Zhang L.: Land



- 1 cover in China, Beijing: Science Press, in Chinese, 2017.
- 2 Xing, L., Tang, X., Wang, H., Fan, W., and Wang, G. Monitoring monthly surface water dynamics of Dongting Lake
3 using Sentinel-1 data at 10 m, PeerJ, 6, e4992, <https://doi.org/10.7717/peerj.4992>, 2018.
- 4 Xu, H.Q.: Modification of normalized difference water index (NDWI) to enhance open water features in remotely
5 sensed imagery, International Journal of Remote Sensing, 27, 3025–3033,
6 <https://doi.org/10.1080/01431160600589179>, 2006.
- 7 Zhang, G., T. Yao, H. Xie, K. Zhang, and F. Zhu. Lakes' State and Abundance across the Tibetan Plateau, Chinese
8 Science Bulletin, 59, 3010–3021, <https://doi.org/10.1007/s11434-014-0258-x>, 2014.
- 9 Zhang, G., Li, J., and Zheng, G.: Lake-area mapping in the Tibetan Plateau: an evaluation of data and methods,
10 International Journal of Remote Sensing, 38, 742–772, <https://doi.org/10.1080/01431161.2016.1271478>, 2017.
- 11 Zhang, T., Ren, H., Qin, Q., Zhang, C., and Sun, Y.: Surface Water Extraction From Landsat 8 OLI Imagery Using the
12 LBV Transformation, IEEE JOURNAL OF SELECTED TOPICS IN APPLIED EARTH OBSERVATIONS AND
13 REMOTE SENSING, 10, 4417–4429, <https://doi.org/10.1109/JSTARS.2017.2719029>, 2017.